

## DETERMINATION OF TRUE RMS EMITTANCE FROM OTR MEASUREMENTS\*

C. F. Papadopoulos<sup>†</sup>, R.B. Fiorito, R. A. Kishek, P. G. O'Shea, A.G. Shkvarunets  
IREAP, University of Maryland, College Park, MD 20742, USA  
M.E. Conde, W. Gai, J.G. Power  
ANL, Argonne, IL 60439, USA

### Abstract

Single foil OTR and two foil OTR interferometry have been successfully used to measure the size and divergence of electron beams with a wide range of energies. To measure RMS emittance, two cameras are employed: one focused on the foil to obtain the spatial distribution of the beam, the other focused to infinity to obtain the angular distribution. The beam is first magnetically focused to a minimum size in directions which are orthogonal to the propagation axis, using a pair of quadrupoles. Then simultaneous measurements of the RMS sizes ( $x, y$ ) and divergences ( $\theta_x, \theta_y$ ) of the beam are made. However, in the process of a quadrupole scan, the beam can go through a spot size minimum, a divergence minimum and a waist, i.e. the position where the cross-correlation term ( $\langle xx' \rangle$  or  $\langle yy' \rangle$ ) is zero. In general, the beam size, divergence and focusing strength for each of these conditions are different. We present new algorithms that relate the beam and magnetic parameters to the RMS emittance for each of these three cases. We also compare the emittances, obtained using our algorithms and measurements made at the ANL AWA facility, with those produced by computer simulation.

### INTRODUCTION

Optical Transition Radiation has been successfully employed in the past for the measurement of the RMS beam size  $x_{\text{rms}} = \sqrt{\langle x^2 \rangle}$  as well as the RMS beam divergence  $\theta_{x_{\text{rms}}} = \sqrt{\langle x'^2 \rangle}$ . Using an appropriate experimental setup, those two quantities can be measured simultaneously. On the other hand, in order to measure the normalized emittance  $\epsilon_n$  given in Eq. (1)

$$\epsilon_n^2 = \beta^2 \gamma^2 (\langle x^2 \rangle \langle x'^2 \rangle - \langle xx' \rangle^2) \quad (1)$$

we also need the cross-correlation term  $\langle xx' \rangle$ , which is not directly measurable by OTR. In this paper we present a novel method that extends the widely used quadrupole and solenoid scan methods to include RMS divergence, as well as RMS size, measurements.

\* Work supported by US DOE of High Energy Physics and Fusion Energy Sciences, and by US DOD Office of Naval Research and Joint Technology Office.

<sup>†</sup> Corresponding author: cfpapado@gmail.com

### EMITTANCE MEASUREMENTS FROM SIZE AND DIVERGENCE DATA

We start by constructing the envelope equation for the RMS divergence in the case of a generalized magnet scan, where the scanning magnet is approximated by a thin lens. The transfer matrix equation, relating the initial position and speed of a particle ( $x_i, x'_i$ ) to their final values ( $x_f, x'_f$ ) are given in Eq. (2).

$$\begin{pmatrix} x_f \\ x'_f \end{pmatrix} = \begin{pmatrix} 1 & L \\ 0 & 1 \end{pmatrix} \times \begin{pmatrix} 1 & 0 \\ -\frac{1}{f} & 1 \end{pmatrix} \times \begin{pmatrix} x_i \\ x'_i \end{pmatrix} \quad (2)$$

where  $f$  is the focal length of the scanning lens and  $L$  is the length of the drift section between the lens and the foil where the beam measurements are taken.

By taking moments of Eq. (2), we can construct the equations for the size, divergence and cross-correlation of the beam:

$$\begin{aligned} \langle x_f^2 \rangle &= \left(1 - \frac{L}{f}\right)^2 \langle x_i^2 \rangle + L^2 \langle x_i'^2 \rangle \\ &\quad + 2L \left(1 - \frac{L}{f}\right) \langle x_i x_i' \rangle \end{aligned} \quad (3)$$

$$\langle x_f'^2 \rangle = \frac{1}{f^2} \langle x_i^2 \rangle + \langle x_i'^2 \rangle - \frac{2}{f} \langle x_i x_i' \rangle \quad (4)$$

$$\begin{aligned} \langle x_f x_f' \rangle &= -\frac{1}{f} \left(1 - \frac{L}{f}\right) \langle x_i^2 \rangle + L \langle x_i'^2 \rangle \\ &\quad + \left(1 - 2\frac{L}{f}\right) \langle x_i x_i' \rangle \end{aligned} \quad (5)$$

By varying the current through the magnet, we change the focal length  $f$  and we are able, in general, to achieve two experimental conditions, a) a minimum spot size and b) a minimum divergence. This allows us to calculate the cross-correlation term in either of those cases, given in Eq. (6) and Eq. (7) respectively.

$$\frac{\partial (\langle x_f^2 \rangle)}{\partial f} = 0 \rightarrow \langle x_f x_f' \rangle = \frac{\langle x_f^2 \rangle}{L} \quad (6)$$

$$\frac{\partial (\langle x_f'^2 \rangle)}{\partial f} = 0 \rightarrow \langle x_f x_f' \rangle = L \langle x_f'^2 \rangle \quad (7)$$

We can now substitute the measured  $x_{\text{rms}}$  and  $\theta_{\text{rms}}$  as well as the calculated value of  $\langle xx' \rangle$  in Eq. (1) and calculate the emittance  $\epsilon_n$ .

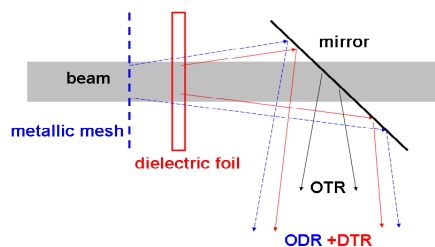


Figure 1: Mesh-dielectric foil transmission interferometer

## THE OTR INTERFEROMETER

Conventional OTRI cannot be used for low emittance beams because scattering in the first foil of the OTR interferometer dominates and obscures the beam divergence ( $1\mu\text{m}$  of Aluminum scatters 8 MeV electrons by RMS  $\theta \sim 5$  mrad). To overcome this problem we have devised a perforated foil (mesh) solid mirror foil reflection interferometer [1, 2, 3] which is useful at moderate beam energies ( $E > 50$  MeV).

For low energy beams the inter foil spacing ( $L \sim \gamma^2 \lambda$ ) is too small to observe the interferences of forward ODR from the mesh and backward OTR from the mirror in a standard reflection geometry. For example, at beam energy  $E = 8$  MeV and  $\lambda = 632\text{nm}$ ,  $L < 1$  mm. To overcome this problem, we have developed a transmission interferometer [4]. This interferometer uses a transparent dielectric foil as a second foil. The forward ODR produced by the mesh passes through the dielectric foil and interferes with forward radiation produced by the dielectric itself. A transport mirror is used to redirect the interfering radiations into the optical measurement system (see Fig. 1).

An optical Diffraction Dielectric foil Transmission Interferometer DDTI was designed and used to measure the electron beam divergence of the Argonne National Labs Advanced Wakefield Accelerator operating at 8 – 14 MeV. The average current of this machine is about  $0.1\mu\text{A}$ , and the repetition rate is 5 Hz.

The codes BEAMDR and CONVD, described in [4], are used to calculate the interference pattern produced by the ODR from the mesh and the dielectric foil radiation. The code CONVD includes the full radiation properties of the dielectric and also takes into account the refraction, reflection, attenuation and phase shift of radiation from the mesh within the dielectric foil. However, the exact values of thickness and refractive index of the dielectric foil are needed for CONVD. In order to find them we record the OTR produced by the 13.8 MeV beam passing through a single metallic foil (metalized kapton) and also we recorded the radiation from interferometer produced by the same beam. Fig. 2 shows the angular distributions of OTR left image and radiation from interferometer right image. Corresponding vertical scans of intensity are shown in Fig. 3 as dashed lines: red interferometer; blue OTR. Fitting of the experimental-dashed lines and theoretical-solid lines (red and blue lines in Fig. 3) allows to find the

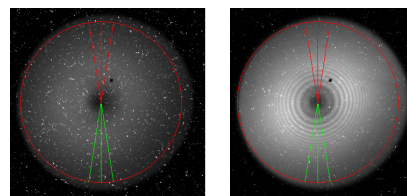


Figure 2: Images of angular distribution of OTR from metallic foil (left) and ODDTI (right) used for kapton foil calibration. Also there are shown the vertical scan sectors.

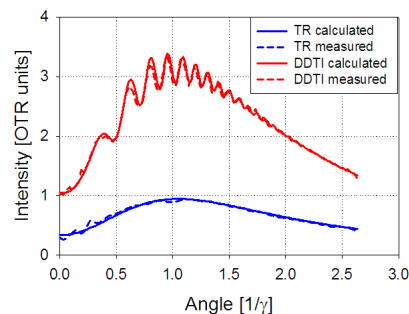


Figure 3: Measured and calculated (the best fit) angular distribution of radiation from metallic foil and interferometer.

beam and interferometer parameters including the thickness of the kapton foil used in the interferometer.

## EMITTANCE MEASUREMENT AT THE AWA FACILITY

During the experiment, a solenoid right after the photocathode gun was used as the scanning magnet, and the interferometer was placed 356 cm from the gun. Due to experimental constraints, we diverted from the idealized solenoid scan, and had to use the RF linac to boost the beam energy from 7.5 MeV at the gun to 13.8 MeV at the interferometer. This had an RF focusing effect [5] on the beam, as illustrated in Fig. 4. Hence, the simplified analysis giving Eq. (6) and Eq. (7) had to be expanded to include linear space charge forces, as well as the RF focusing effect from the linac. For this reason, we constructed a fast envelope code that included these effects. Comparisons of this code with Tstep showed good agreement, as shown in Fig. 5

### Comparison of Scan Data with Model

The size and divergence data taken at AWA are given in Table 1 Using the fast envelope code, we were able to scan a three dimensional parameter space to find the initial size, divergence and emittance that best fitted the data. The best fit in the  $x$  and  $y$  directions is shown in Figs. 6(a), 6(b) and it corresponds to normalized emittance values of  $\epsilon_x = 19\text{mm-mrad}$  and  $\epsilon_y = 22\text{mm-mrad}$ . Independent measurements of the emittance at AWA [6] give an emit-

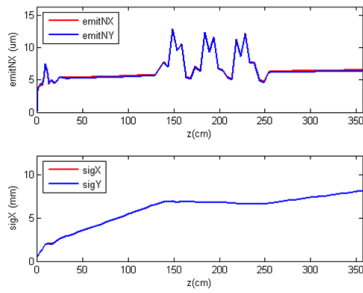


Figure 4: Tstep simulation of the evolution of normalized emittance ( $\epsilon_{nx}$  and  $\epsilon_{ny}$ , upper) and the beam envelope in  $x$  and  $y$  (lower). Note the effect of the linac (situated between 128.5 and 255 cm) in both the emittance and the size of the beam.

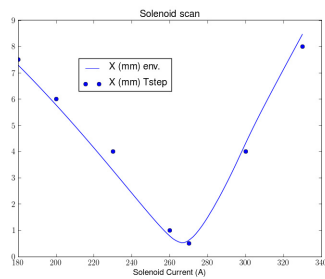


Figure 5: Comparison of solenoid scan between Tstep (points) and envelope code (solid line)

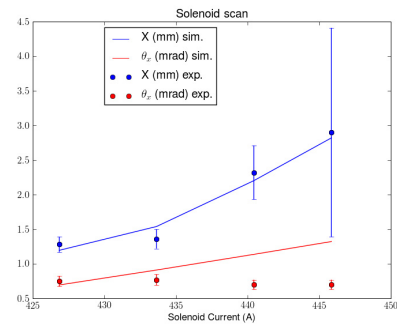
tance value in the range 9 – 12 mm-mrad. The discrepancy between the two experimental methods is presently under investigation and thought to be related to the shot-to-shot noise, as well as the presence of the linac.

## CONCLUSION

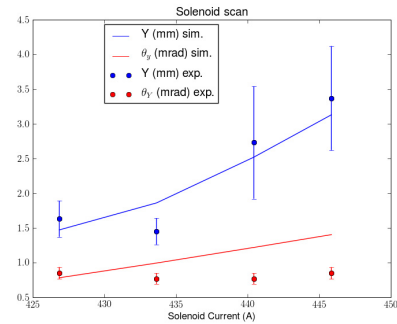
We present a novel method for the measurement of emittance that takes advantage of the ability of OTR interferometry to simultaneously measure the RMS size and RMS divergence of a beam. In particular, we used a solenoid scan to approach a beam size minimum, and fitted both the size and divergence data in order to get the beam emittance in the  $x$  and the  $y$  directions. Comparison with pepperpot

Table 1: Measured size and divergence of the beam for a solenoid scan

Solenoid Current (A)	X size (mm)	$\theta_x$ (mrad)	Y size (mm)	$\theta_y$ (mrad)
427	1.28	0.75	1.63	0.85
434	1.36	0.77	1.45	0.77
440	2.32	0.7	2.73	0.77
445	2.9	0.7	3.37	0.85



(a)  $\epsilon_x$  fit



(b)  $\epsilon_y$  fit

Figure 6: Comparison of simulation (solid line) and experimental (points) data for the  $x$  (up) and  $y$  (down) emittance

scans at the same conditions gives an emittance  $\sim 40\%$  smaller, likely because the presence of the linac complicated the analysis of the solenoid scan.

## REFERENCES

- [1] A. Shkvarunets, R. Fiorito, and P. O'Shea, "Optical diffraction-transition radiation interferometry and its application to the measurement of beam divergence," *Nuclear Inst. and Methods in Physics Research, B*, vol. 201, no. 1, pp. 153–160, 2003.
- [2] R. B. Fiorito, A. G. Shkvarunets, T. Watanabe, V. Yakimenko, and D. Snyder, "Interference of diffraction and transition radiation and its application as a beam divergence diagnostic," *Phys. Rev. ST Accel. Beams*, vol. 9, p. 052802, May 2006.
- [3] R. Fiorito, A. Shkvarunets, and P. O'Shea, "Measurement of electron beam divergence using OTR-ODR interferometry," in *Particle Accelerator Conference, 2003. PAC 2003. Proceedings of the*, vol. 4, 2003.
- [4] A. Shkvarunets, R. Fiorito, P. O'Shea, J. Power, M. Conde, and W. Gei, "Optical diffraction-dielectric foil radiation interferometry diagnostic for low energy beams," in *IEEE Particle Accelerator Conference, 2007. PAC*, pp. 4012–4014, 2007.
- [5] J. Rosenzweig and L. Serafini, "Transverse particle motion in radio-frequency linear accelerators," *Physical Review E*, vol. 49, no. 2, pp. 1599–1602, 1994.
- [6] J. G. Power, M. Conde, W. Gai, F. Gao, W. Liu, Z. Yusof, and P. R. Piot, "Measurement of the 4D Transverse Phase Space Distribution from an RF Photoinjector at the AWA,"